Bioorganic & Medicinal Chemistry 17 (2009) 1701–1708

Contents lists available at ScienceDirect

Bioorganic & Medicinal Chemistry

journal homepage: www.elsevier.com/locate/bmc

Identification of tripeptides recognized by the PDZ domain of Dishevelled

Ho-Jin Lee [a], Nick X. Wang [a], Youming Shao [a], Jie J. Zheng [a,b,*]

[a] Department of Structural Biology, St. Jude Children's Research Hospital, 262 Danny Thomas Place, Memphis, TN 38105, USA
[b] Department of Molecular Sciences, The University of Tennessee Health Science Center, Memphis, TN 38163, USA

ARTICLE INFO

Article history:
Received 31 October 2008
Revised 18 December 2008
Accepted 19 December 2008
Available online 3 January 2009

Keywords:
Binding free energy
Protein–ligand interaction
Ligand computational screening
NMR
Fluorescence spectroscopy

ABSTRACT

The development of inhibitors of Dishevelled (Dvl) PDZ protein–protein interactions attracts attention due to a possible application in drug discovery and development. Using nuclear magnetic resonance (NMR) spectroscopy, we found that a tripeptide VVV binds to the PDZ domain of Dvl, which is a key component involved in Wnt signaling. Using a computational approach calculating the binding free energy of the complexes of the Dvl PDZ domain and each of the tripeptides VXV (X: any amino acid residue except Pro), we found that a tripeptide VWV had the highest binding affinity. Consistent with the computational result, experimental results showed that the binding of the tripeptide VWV to the Dvl PDZ domain was stronger than that of the tripeptide VVV. The binding affinity of the tripeptide VWV was comparable to that of the organic molecule NSC668036, which was the first identified Dvl PDZ inhibitor. The three-dimensional structure of the complex Dvl1 PDZ/VWV was determined to investigate the role of the energetically favorable W(−1) residue in binding. These interactions were also explored by using molecular dynamic simulation and the molecular mechanics Poisson–Boltzmann surface area method. Taken together, these two tripeptides may be used as modulators of Wnt signaling or as a scaffold to optimize an antagonist for targeting Dvl1 PDZ protein–protein interaction.

1. Introduction

Dishevelled (Dvl) proteins function in cell differentiation and apoptosis through Wnt signaling pathways.[1,2] Overexpression of Dvl showing activation of canonical Wnt signaling has been reported in several types of cancer cells and tissues.[3–5] These findings suggest that discovery of small molecules or peptides modulating the function of Dvl proteins in Wnt signaling would be valuable in understanding biological processes and developing a potential drug.[3] Dvl proteins have three domains that are highly conserved in the animal kingdom, including the DIX, PDZ, and DEP domains.[1,6–10] Among these domains, the Dvl PDZ domain, which is a protein–protein interaction module, has been identified as a potential target for drug discovery and development.[9,11] The Dvl PDZ domain is ~100 amino acids long and comprises six β-strands (βA to βF) and two α-helices (αA and αB); the Dvl1 PDZ domain recognizes an internal sequence and an extreme C-terminal tail of target proteins through a binding groove formed between the αB-helix and βB-strand.[9,12,13] A peptide bound to Dvl1 PDZ domain forms an additional β-strand structure.[12] Notably, the Dvl1 PDZ-bound peptide attenuates the Wnt/β-catenin signaling induced by Wnt1.[9] This discovery inspired us and others to explore small-molecule inhibitors of Dvl PDZ protein–protein interaction.[14–16]

In addition to the development of small molecules, we are also investigating short peptides targeting the Dvl PDZ domain for a possible application in peptide-based therapeutics.[17] Despite the disadvantages of peptide drugs, such as their high price and low bioavailability, they are of continued interest because they are more target-specific and less toxic than small molecules.[17] Natural peptides and synthetics derived from bioactive peptides have actually been used for the prevention and treatment of diseases.[17,18]

Tripeptides are drawing especially great attention in drug discovery because they are easy to modify and small (M.W. < 500 Da), which is consistent with typical small-molecule bioavailable oral drugs.[19–24] In addition, the conformational properties of tripeptides have been explored to allow an understanding of the protein folding and intrinsic properties of amino acid residues in protein structures.[25–30] Recent studies revealed that even short peptides could adopt a specific conformation in gas phase or in water solution, implying that they might serve as a model as well as a molecular scaffold for future drug design.[25–30]

Using nuclear magnetic resonance (NMR) spectroscopy, we found that the tripeptide VVV interacts directly with the Dvl PDZ

Abbreviations: NMR, nuclear magnetic resonance; HSQC, heteronuclear single-quantum coherence; NOE, nuclear Overhauser enhancement spectroscopy; MM-PBSA, molecular mechanics Poisson–Boltzmann surface area; RMSD, root-mean-square deviation.

* Corresponding author. Tel.: +1 901 595 3168; fax: +1 901 595 3032.
E-mail address: jie.zheng@stjude.org (J.J. Zheng).

0968-0896/$ - see front matter © 2008 Elsevier Ltd. All rights reserved.
doi:10.1016/j.bmc.2008.12.060

domain. After confirming the binding, we optimized a peptide to enhance the binding affinity to the Dvl PDZ domain using an approach that combines computational biology, peptide chemistry, and structural biology. To understand the binding mechanism, we determined the three-dimensional structure of the complex and Dvl1 PDZ/tripeptide VWV using NMR-derived information. We also conducted molecular dynamic (MD) simulations and the molecular mechanics Poisson–Boltzmann surface area method (MM-PBSA) calculation to reveal the difference between the two peptides in their binding affinities to the Dvl PDZ domain.

2. Results and discussion

2.1. Tripeptide VVV recognizes the Dvl1 PDZ domain

To discover and optimize a Dvl PDZ-binding peptide, we chose the tripeptide VVV as a model because it has been reported to predominantly sample a β-strand structure in water solution[25,31] and it resembles the PDZ-binding motif, such as S/T-X-Φ and Φ-X-Φ (X: any amino acid; Φ: hydrophobic residue).[32] To probe the interaction between the tripeptide VVV and the Dvl1 PDZ domain, we used NMR spectroscopy. The interaction of a protein and a short peptide can be easily detected by the chemical shift perturbations or peak broadening upon adding the unlabeled peptide to the ^{15}N-labeled targeted protein.[33] Figure 1A shows the ^{1}H–^{15}N-HSQC spectra of the ^{15}N-labeled Dvl1 PDZ domain with titration of the unlabeled tripeptide VVV, indicating a direct interaction. The large chemical shift perturbations resulting from the binding of the tripeptide VVV to the Dvl1 PDZ domain were observed for residues Ile264 and Ser265 in the βB-strand and the residues Arg322 and Val325 on the αB-helix structure of the Dvl1 PDZ domain (Fig. 1B). These peaks showed the continuous changes in chemical shifts in the ^{1}H–^{15}N-HSQC spectra as the concentration of the tripeptide VVV was increased, indicating that its interaction is in the fast exchange range on the NMR time scale. The worm representation of the backbone structure of the Dvl1 PDZ domain based on the chemical shift perturbation data in Figure 1C demonstrates that the tripeptide VVV binds to the αB/βB-binding groove of the Dvl1 PDZ domain as expected.

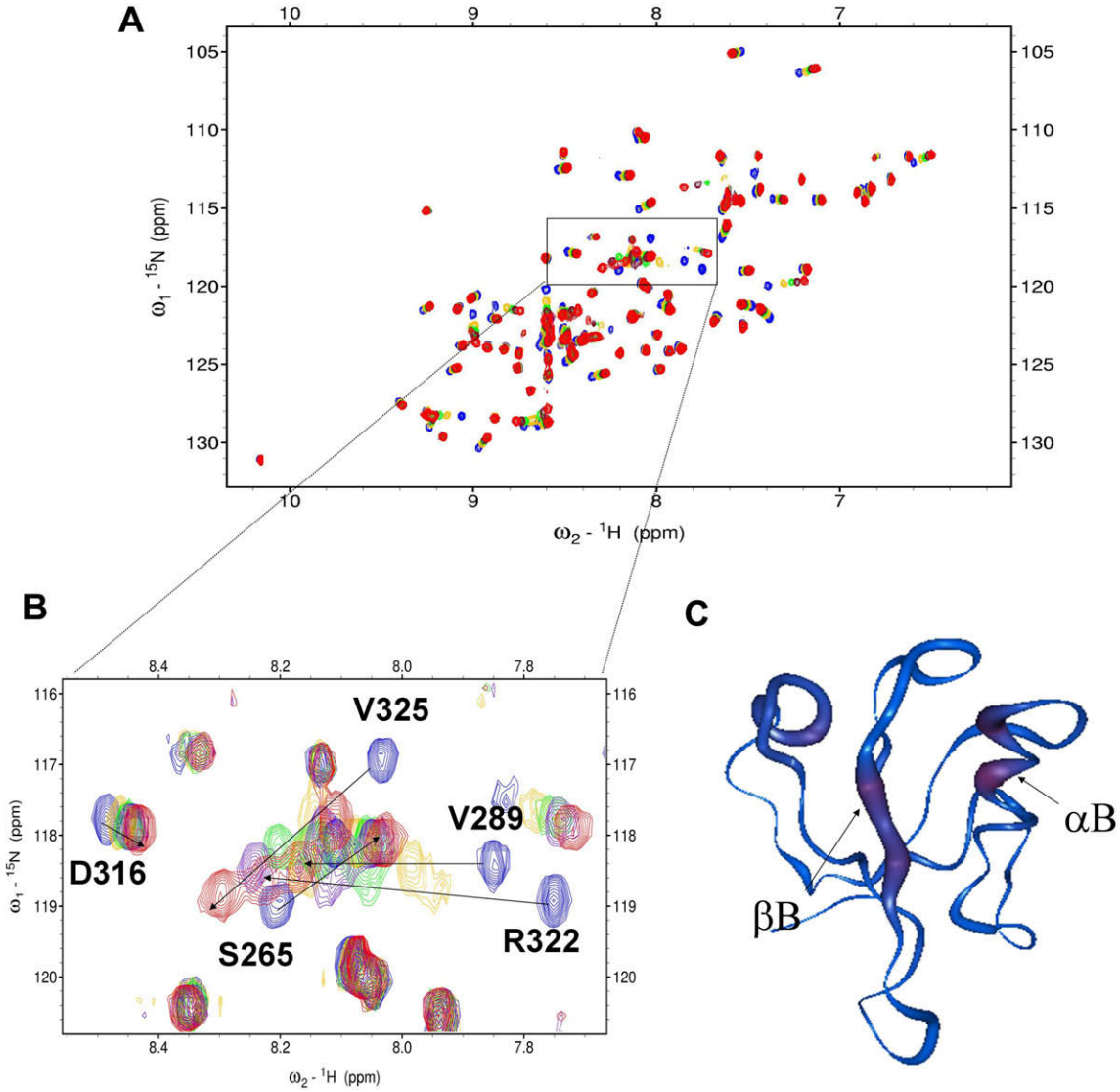

Figure 1. Tripeptide VVV interacts with the Dvl1 PDZ domain. (A) ^{15}N-HSQC spectra of ^{15}N-labeled Dvl1 PDZ domain alone (0.3 mM, blue) and with varying concentrations of tripeptide VVV. (B) The extended ^{15}N-HSQC spectra of the Dvl1 PDZ domain as a function of the tripeptide VVV concentration (blue: free, gold 1:4; green: 1:7; purple 1:11, red 1:22). (C) The worm representation of the backbone structure of the Dvl1 PDZ domain. The thickness and color of the worm is proportional to the weighted sum of the proton and amide chemical shift perturbations upon binding of peptide VVV (red, high; blue, low). The program Insight II was used to prepare (C).

2.2. Evaluation of the binding free energy of the complex of Dvl1 PDZ and model tripeptide VXV

The observation of the direct interaction between the tripeptide VVV and the Dvl PDZ domain prompted us to investigate whether other similar tripeptides could bind to the Dvl PDZ domain. Because the tripeptide VVV resembles the typical PDZ-binding motif, investigating the role of a particular amino acid residue in binding was expected to provide valuable information to optimize a peptide bound to the Dvl1 PDZ domain. Because the P(−1) residue in the PDZ-binding peptide (position 0 referring to the extreme C-terminal residue) has been found to play a role in enhancing binding in several cases,[34–36] we virtually evaluated the binding affinities of Dvl PDZ with model tripeptides VXV (X: any amino acid residue except Pro) using the ICM empirical binding energy function (ICM Pro ver. 3.2).[37] In this study, we used X-ray crystallographic data of the structure of the *Xenopus* Dishevelled PDZ (Xdsh PDZ)/Dapper peptide (SGSLKLMTTV) complex (PDB code: 1L6O:A).[12] We used the coordinates of the last three amino acid residues (TTV) for the Dapper peptide in the complex structure to generate the model tripeptides. We assumed that all tripeptides bound to the PDZ domain adopt the β-strand that resemble the bound conformation of the Dapper peptide.[12] The side chain of each modeled tripeptide in the complex was optimized to escape a possible collapse of the side chain between Xdsh PDZ and the VXV tripeptide before calculating the binding free energy of the complex. Figure 2 shows the relative binding free energy ($\Delta\Delta G_{binding}$) of the Xdsh PDZ and model tripeptide VXV with respect to the tripeptide VVV ($\Delta G_{binding}$ is −21.8 ± 3.3 kcal/mol). Notably, the tripeptide VWV had the highest binding energy to the PDZ domain of Xdsh. Although the ICM empirical binding energy function has been validated for several cases,[37] we wondered whether this would be the case for our model system. To confirm the theoretical result, we used an NMR-binding assay.

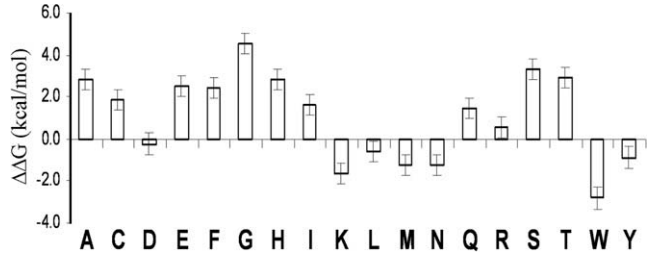

Figure 2. Tripeptide VWV had the highest binding energy. The relative binding energies ($\Delta\Delta G_{binding}$) of *Xenopus* Dsh PDZ and model tripeptides VXV with respect to the tripeptide VVV. The energies were calculated by using the ICM empirical binding energy function (X represents any amino acid residue except Pro).

2.3. Tripeptide VWV indeed binds to the Dvl PDZ domain

We chemically synthesized the tripeptide VWV and explored its interaction with the Dvl1 PDZ domain using NMR spectroscopy. Figure 3A shows the fingerprint region of the ^{1}H–^{15}N-HSQC spectra of the ^{15}N-labeled Dvl1 PDZ domain with varying concentrations of unlabelled tripeptide VWV. Surprisingly, the residues I264, R322, and V325 began to disappear upon stepwise addition of the tripeptide VWV and reappeared at the saturated concentration. This indicates that the complex formation is in the intermediate exchange range on the NMR time scale. The two largest chemical shift perturbations were found in residues I264 ($\Delta\delta_{total}$ = 0.565 ppm) on the βB-strand and R322 ($\Delta\delta_{total}$ = 0.497 ppm) on the αB-helix of Dvl1 PDZ at the saturated concentration. They are much larger than the chemical shift perturbations in the same residues caused by the binding of the VVV peptide (Figs. 1B and 3A), indicating that the VWV peptide binds to the PDZ domain tighter than the VVV peptide.

We next determined the binding affinity (K_D) of tripeptides using fluorescence spectroscopy (Table 3). In this study, we made a fluorescence-labeled PDZ domain, 2-((5(6)-tetramethylrhodamine)carboxylamino)ethylethanethiosulfonate (TMR)-PDZ domain of Dvl1 (Fig. 4).[14] The fluorescence intensity of the TMR-PDZ domain at 597 nm was monitored while the tripeptide VVV or VWV was added. The K_D value was calculated from a reciprocal plot of fluorescence intensity quenching against the concentration of the peptide. The result showed that the binding affinity of the tripeptide VWV was 2 μM and that of the tripeptide VVV was 71 μM for the TMR-PDZ domain, which supports the ICM theoretical result that modification of the P(−1) position in the tripeptide can increase the binding affinity for the Dvl1 PDZ domain. Notice that the K_D values of the tripeptides are much lesser than that of the organic molecule NSC668036, which was the first identified antagonist for targeting Dvl1 PDZ protein interactions.[14] Using the same binding assay, the K_D value of NSC668036 and TMR-PDZ was found to be 237 ± 31 μM.[14]

2.4. Structures of the complex between the Dvl PDZ domain and the VWV peptide

To understand the greater affinity of the tripeptide VWV than of the tripeptide VVV for binding to the Dvl1 PDZ domain, we determined the three-dimensional structure of the Dvl1 PDZ/VWV complex. The assigned intermolecular nuclear Overhauser effects (NOEs) between tripeptide VWV and the Dvl1 PDZ domain are summarized in Figure 5A and Table 1. In the complex structure cal-

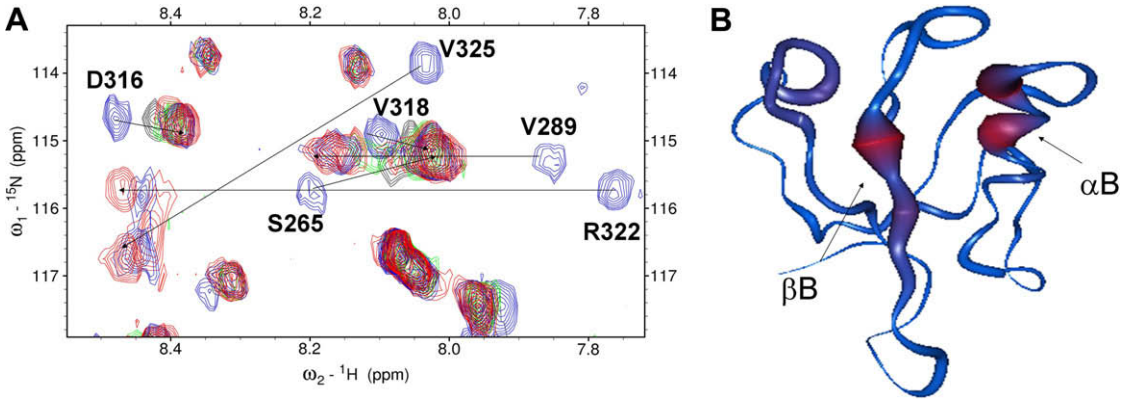

Figure 3. Direct interaction of the tripeptide VWV and the Dvl1 PDZ domain. (A) The extended ^{15}N-HSQC spectra of the Dvl1 PDZ domain at various concentration of tripeptide VWV (blue: free, cyan 1:1, green 1:3, purple 1:5, red 1:8). (B) The worm representation of the backbone structure of the Dvl1 PDZ domain. The thickness of the worm structure was normalized by the chemical shift perturbation datum of the I264 residue in Figure 1.

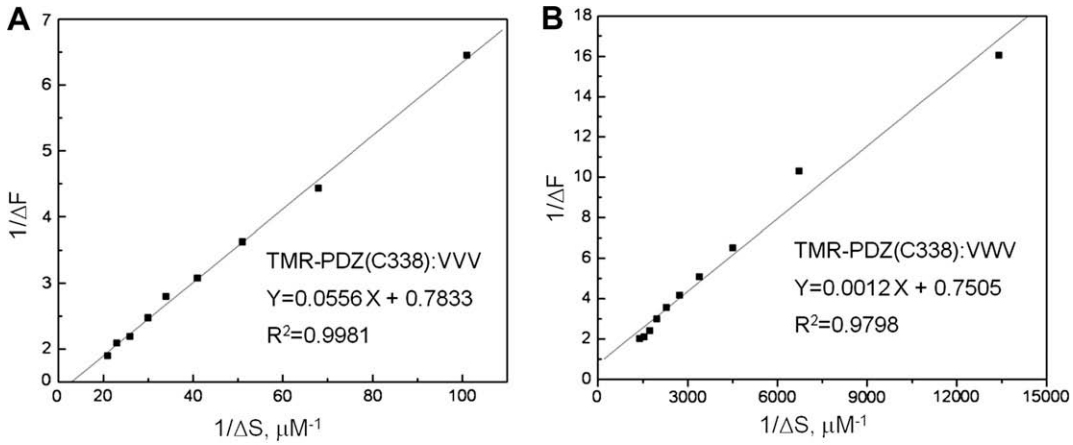

Figure 4. A reciprocal plot of fluorescence intensity quenching (ΔF) of the TMR-PDZ(C338) domain of Dvl1 against the concentration (ΔS) of the tripeptides (A) VVV and (B) VWV.

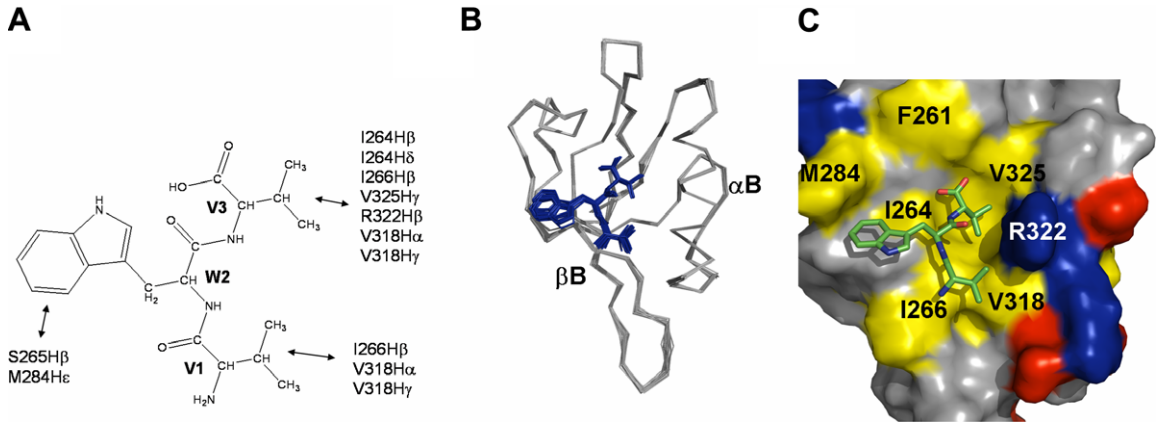

Figure 5. Structures of the Dvl1 PDZ/VWV complex. (A) Summary of intermolecular NOEs between the tripeptide VWV and the Dvl1 PDZ domain. (B) The ensemble of the 20 lowest energy conformations of the Dvl1 PDZ/VWV complex. (C) The lowest energy conformation of the Dvl1 PDZ/VWV complex. Surface representation shows the binding interface between the Dvl1 PDZ domain and the VWV tripeptide. The hydrophobic amino acid residues in the Dvl1 PDZ domain surface model are drawn in yellow, the positively charged residues in blue, the negatively charged residues in red, and the uncharged polar residues in gray. The bound VWV tripeptide is shown in the stick model. The program Pymol was used to prepare the figures.

culation, a total of 26 experimental restraints were used, including 22 intermoleulcar NOEs between the peptide and the protein and 4 intramolecular NOEs from the tripeptide VWV bound to the PDZ domain. The 20 lowest energy conformations were selected from the 100 water-refined complexes for further structural analysis (Fig. 5B). The statistical result of the complex is summarized in Table2. Not surprisingly, the tripeptide VWV was fitted into the hydrophobic pocket of the Dvl1 PDZ domain and formed an additional β-strand with respect to the βB-structure (Fig. 5B). The lowest energy conformation of the PDZ/VWV complex is shown in Figure 5C: the side chains of P(0) and P(−2) contacted the hydrophobic residues (color code: yellow) within the binding site of the Dvl1 PDZ domain. The side chain of the P(−1) residue in the tripeptide was oriented to the βB- and βC-strand regions of the Dvl1 PDZ domain. The amino acid residues of the Dvl1 PDZ domain in proximity (<4.0 Å) to tripeptide V(−2)–W(−1)–V(0) were as follows: the residues Leu262, Gly263, Ile264, Val325, Arg322, Leu321, and Val318 were close to the residue V(0); the residues Ile266 and Val318 were close to the residue Val(−2); and Ser265 and Met284 were close to the W(−1) residue (Fig. 5C). The solution structure of the PDZ/VWV complex was in a good agreement with the complex structure used for the ICM calculations (data not shown).

The structure of the PDZ/VWV complex implies that the difference in the binding affinity for the tripeptides VVV and VWV may result from the hydrophobic interaction between the side chain of the Ser265 or Met284 residues and the Trp side chain in the P(−1) position of the tripeptide VWV. However, it is difficult to quantitatively explain the linkage between the binding affinity of the tripeptide and the Dvl1 PDZ domain with the structural information.

2.5. Molecular dynamics simulation and MM-PBSA calculation for the complexes of Dvl1 PDZ with tripeptides VVV and VWV

To further understand the difference in the binding energies for the two complexes, we performed an MD simulation using AMBER8 software.[38] The starting structures of the complexes used were the lowest energy conformation as described in the Materials and Methods section. MD simulations were performed in explicit water for 2 ns. To analyze the stability of the MD simulations, we plotted the root-mean-square deviation (RMSD) values relative to the initial structures of the PDZ backbone atoms during the 2 ns MD simulation against time (Fig. 6). The complexes of the Dvl1 PDZ domain with the VVV or VWV tripeptide reached convergence quickly and remained stable thereafter. We then calculated the binding free energy of the interaction between the Dvl1 PDZ domain and the tripeptides for the last 1 ns with the MM-PBSA method.[39,40] The individual energy terms that contribute to binding free energy are listed in Table 3. The predicted binding free energy (ΔG)

Table 1
Intermolecular NOEs between the Dvl1 PDZ domain and the tripeptide V1(−2)–W2(−1)–V3(0)

Assignments	ω1	ω2	ω3	Relative NOE intensity[a]
V1Hβ-I266Cδ1-Hδ1	1.965	10.416	0.417	w
V1Hβ-I266CB-Hβ	1.932	36.188	1.553	w
V1Hβ-I266CG2-Hγ2	1.967	15.579	0.464	m
V1Hγ2-I266CB-Hβ	0.659	36.254	1.554	w
V1Hγ2-V318Cα-Hα	0.650	24.194	3.212	m
V1Hγ1-V318Cγ1-Hγ1	0.635	20.565	0.936	m
$W2H_{ring}$-S265Cβ-S265Hβ2	7.282	22.563	3.589	m
$W2H_{ring}$-S265Cβ-S265Hβ3	7.289	22.591	3.399	m
$W2H_{ring}$-S265Cβ-S265Hβ2	7.027	22.600	3.591	s
$W2H_{ring}$-S265Cβ-S265Hβ3	7.018	22.576	3.397	s
$W2H_{ring}$-M284Cε-Hε	7.288	14.116	1.467	w
$W2H_{ring}$-M284Cε-Hε	7.032	14.101	1.467	m
V3Hβ-V318Cγ1-Hγ1	1.787	20.584	0.937	m
V3Hγ2-L262Cβ-Hβ	0.628	39.300	1.623	m
V3Hγ2-I264Cβ-Hβ2	0.633	39.104	1.850	m
V3Hγ2-I264Cδ1-Hδ1	0.628	10.031	0.376	m
V3Hγ2-I266Cγ1-Hγ11	0.639	22.744	1.246	s
V3Hγ2-I266Cγ1-Hγ12	0.634	22.763	0.916	m
V3Hγ2-I266Cγ2-Hγ2	0.633	15.568	0.464	m
V3Hγ1-R322Cβ-Hβ	0.665	27.324	1.838	w
V3Hγ2-V318Cγ2-Hγ2	0.632	19.344	0.303	w
V3Hγ2-V325Cγ1-Hγ1	0.629	19.122	0.883	m

Data were obtained from a 3D ^{13}C-F1-half-filtered F2-edited NOESY–HSQC experiment (mixing time = 200 ms) at 10 °C in 0.1 M phosphate buffer, 0.5 mM EDTA, pH 7.5.

[a] NOE cross-peak intensities were classified as strong, medium, weak, and very weak, and assigned to restraints of 1.8–3.0 Å, 1.8–4.0 Å, 1.8–5.0 Å, 1.8–6.0 Å, respectively, with appropriate pseudoatom corrections.

Table 2
Structural statistics of the 20 lowest energy structures of Dvl1 PDZ/VWV complex

	PDZ-VWV
Number of unambiguous interaction restraints	
Intramolecular NOEs	4
Intermolecular NOEs	22
RMSD deviation from the averaged coordinates[a]	
All backbone (Å)	0.31 ± 0.03
All heavy atom (Å)	0.53 ± 0.04
Overall energy of the 20 lowest energy conformations	
E_{total} (kcal/mol)	−117.9 ± 3.2
E_{vdw} (kcal/mol)	−30.8 ± 1.6
E_{elec} (kcal/mol)	−87.1 ± 1.3
E_{NOE} (kcal/mol)	0.03 ± 0.01
Buried surface of the 20 lowest energy conformations (Å)^2	653.6 ± 15.6

[a] Calculated from the program MOLMOL.

Table 3
The binding affinity of the complex from MD simulations (MM-PBSA calculation)[a]

Thermodynamic parameters	Dvl1 PDZ/VVV	Dvl1 PDZ/VWV
ΔH	−23.48(0.39)[d]	−30.07(0.41)
E_{ele}(solute)	−70.53(1.10)	−74.76(1.00)
E_{ele}(solvent)	77.20(0.93)	84.32(0.81)
$E_{ele+PB} = E_{ele}$(solute) + E_{ele}(solvent)	6.67	9.56
E_{vdw}	−25.80(0.19)	−34.69(0.23)
$H_{trans/rot}$	−1.78	−1.78
E_{no_pol}	−4.35(0.31)	−4.94(0.01)
ΔTS	−19.74(0.74)	−24.70(1.13)
[b]ΔG	−5.52(0.84)	−7.15(1.20)
[c]ΔG	−5.56	−7.64

[a] In kcal/mol.
[b] MM-PBSA calculation.
[c] From fluorescence experiment, K_D of the TMR-PDZ and tripeptide. $\Delta G^o = 2.303\,RT(\log K_D)$, $R = 1.987$ cal K^{-1} mol^{-1}, $T = 293$ K.
[d] Standard errors of mean in parenthesis.

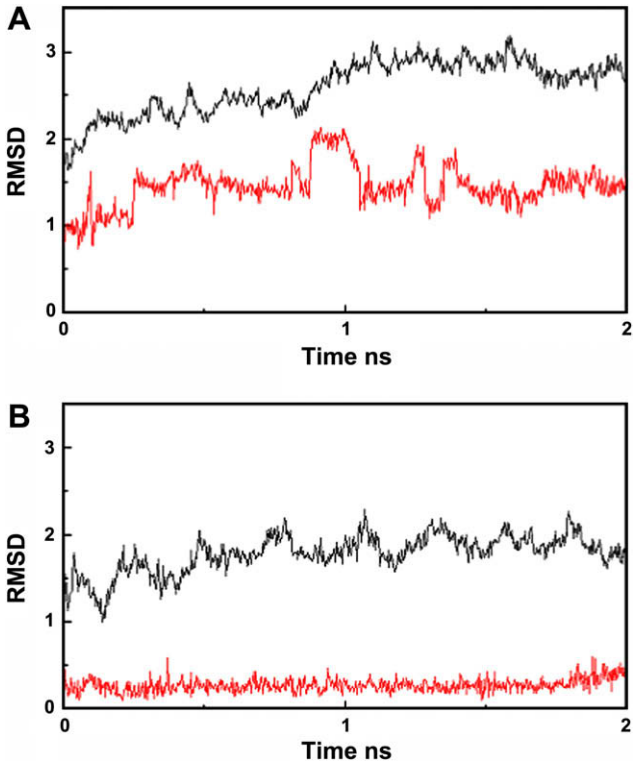

Figure 6. The backbone root-mean-square deviation (RMSD) relative to the initial structures of the backbone atoms and ligand atoms in the (A) Dvl1 PDZ/VVV and (B) Dvl1 PDZ/VWV complexes during a 2-ns molecular dynamics simulation. The black lines represent the backbone RMSDs of the PDZ proteins, and the red line represents the backbone RMSD of the peptides.

of the Dvl1 PDZ/VVV complex was −5.52 ± 0.80 kcal/mol and that of the Dvl1 PDZ/VWV complex was −7.15 ± 1.20 kcal/mol, indicating that the binding of the tripeptide VWV to the Dvl1 PDZ domain is stronger than that of the tripeptide VVV. The relative binding free energies obtained from MM-PBSA calculations were in good agreement with experimental results ($\Delta G = -5.56$ kcal/mol for TMR-PDZ/VVV and $\Delta G = -7.64$ kcal/mol for TMR-PDZ/VWV; Table 3). Besides ranking the binding free energies correctly, MM-PBSA allowed us to break down the total binding free energy into individual components, which enabled us to understand the binding interactions in detail. In Table 3, the $E_{elec+PB}$ is the total electrostatic contribution, including solute–solute and solute–solvent interactions, and E_{vdw} is the van der Waals contribution to the binding. As seen in Table 3, the E_{vdw} favors interaction of the Dvl1 PDZ domain with tripeptide VWV by 8.89 kcal/mol, whereas the electrostatic contribution resists the binding between the Dvl1 PDZ and VWV by 2.89 kcal/mol. The differences between the binding free energy of the two complexes therefore are largely controlled by the van der Waals contribution. This correlates well with the observation that the indole ring of the Trp(−1) residue in the tripeptide was close to the side chain of the S265 and M284 residues. The entropy contribution ($T\Delta S$) disfavors the binding of the PDZ/VWV due to orientational and positional restraints imposed by the larger side chain of the Trp residue; however, the overall binding free energy (ΔG) still promotes the binding of the PDZ/VWV complex over that of the PDZ/VVV complex.

3. Conclusion

In this study, we identified the tripeptides VVV and VWV as Dvl1 PDZ-binding partners using NMR spectroscopy and other methods. The experimental and theoretical results provided evidence that a

single modification at the P(−1) residue in the Dvl1 PDZ-binding peptide can increase the binding affinity through the hydrophobic interaction contribution. Because the binding ability of the tripeptide VWV was comparable to that of the organic compound NSC668036, the first Dvl1 PDZ antagonist identified by the virtual screening and NMR method,[14] the result implies that the tripeptide VWV may serve as a modulator of Dvl PDZ protein interactions or as a molecular scaffold for the design of a new peptidomimetic compound.[41] It can also be proposed that short peptides containing the motif VWV at the C-terminus are potential Dvl PDZ inhibitors. Further studies of the effect of the tripeptide VWV on Wnt signaling should yield valuable information regarding the function of Dvl in embryonic development and malignant diseases. Because numerous PDZ domains are found in the animal kingdom, we cannot rule out the possibility of the tripeptide binding to other PDZ domains.[42–44] To obtain a more selective inhibitor of Dvl PDZ protein–protein interaction, processes similar to those described here are under way to optimize the residues at the −2 and −3 positions of the PDZ-binding ligands that also may influence PDZ-binding affinities significantly.

4. Materials and methods

4.1. Purification of the ^{13}C, ^{15}N-labeled mouse Dvl1 PDZ domain for NMR spectroscopy

The detailed methods for protein production have been described elsewhere.[9] In brief, the cDNA of the mouse Dishevelled1 (Dvl1) PDZ domain (amino acids 251–341) was sub-cloned into the pET28a vector. To improve the protein solubility and to prevent dimerization, Cys338 was replaced with Ala for NMR study. The protein was expressed in BL21(DE3)-codon plus RP *Esherichia coli* cells. The transformed *E. Coli* BL21(DE3) cells were grown at 37 °C in MOPS-containing medium supplemented with $^{15}NH_4Cl$ (1 g/L) and/or ^{13}C-glucose (3 g/L) as the sources of nitrogen and carbon. Protein expression was induced by the addition of 1 mM isopropyl-1-thio-β-D-galactoside (IPTG) until the optical density at 600 nm of the cells was about 0.5. Cells were lysed by microfluidization, and the protein was purified with a HiTrap Chelating HP column of $NiCl_2$ (Amersham Pharmacia Biotech). The column was washed with 20 mM imidazole, followed by 200 mM imidazole (pH 7.8) with 300 mM NaCl. The Dvl1 PDZ domain was further purified by gel filtration on Sephadex G75 in 0.1 M phosphate buffer, pH 7.5, with 0.5 mM EDTA.[9]

4.2. Peptide synthesis and purification

Tripeptide VVV (NSC35938) was obtained from the National Cancer Institute and used without purification. The tripeptide VWV was chemically synthesized by the Hartwell Center for Bioinformatics & Biotechnology at St. Jude Children's Research Hospital and purified by reverse-phase high-performance liquid chromatography. $[M+H]^+$(calcd) = 402.5, $[M+H]^+$(observed) = 403.4 for the VWV peptide.

4.3. NMR spectroscopy and NMR titration experiment

The NMR experiments were performed at 25 °C using a Varian INOVA 600 MHz spectrometer and a Bruker Avance 800 MHz spectrometer equipped with a triple resonance, triple axis actively shielded gradient cold probe. All NMR spectra were processed with the program NMRpipe[45] and analyzed using the program SPARKY 3 (T.D. Goddard and D.G. Kneller, University of California, San Francisco). The interaction between protein and peptide was directly monitored by collecting the ^{15}N-HSQC spectra of ~0.3 mM ^{15}N-labeled protein at varying concentrations of tripeptides in 0.1 M phosphate buffer (pH 7.5) at 298 K. Chemical shift perturbations ($\Delta\delta_{total}$) of ^1H and ^{15}N resonances were obtained and weighted according to Eq. 1:

$$\Delta\delta_{total} = [(\delta^1H)^2 + (\delta^{15}N \times 0.2)^2]^{1/2} \quad (1)$$

4.4. The binding free energy for the Dvl1 PDZ/tripeptide complexes by ICM software

The binding free energy between model tripeptide VXV with the Dvl1 PDZ domain was calculated by using the ICM empirical binding function (X: any amino acid residue). The starting structures of the Dvl1 PDZ/tripeptide complex were generated using the coordinates from the X-ray crystallographic data of the complex structure of *Xenopus* Dishevelled PDZ (Xdsh PDZ) and Dapper peptide (SGSLKLMTTV) (PDB code: 1L6O) using the program SYBYL 7.3 (Tripos Inc.). Hydrogen atoms were added to the model complex structure using SYBYL. Before calculating the binding free energy of the complex, the side chain of each modeled tripeptide in the complex was optimized to escape a possible collapse of the side chain between Xdsh PDZ and its binding partner using the default method provided by the ICM software. The binding free energy of the model tripeptide VXV and Xdsh PDZ was calculated using Eq. 2:

$$\Delta G_{binding} = \Delta G_{vw} + \Delta G_{hb} + \Delta G_{to} + \Delta G_{el} + \Delta G_{sf} \quad (2)$$

Here, ΔG_{vw} is Van der Waals energy, which is defined as nonbonded interatomic pairwise interactions; ΔG_{hb} is hydrogen bonding energy, which is a different form of the 'vw' term for hydrogen bonding donors and acceptors; ΔG_{to} is torsional energy, or dihedral angle deformation energy; ΔG_{el} is electrostatic energy; and ΔG_{sf} is the surface energy, which is surface tension as a product of atomic accessibilities of the total solvent-accessible area. We calculated the binding free energy of the complexes twice independently and averaged the values.

4.5. Fluorescence spectroscopy

A FluoroLog-3 spectrofluorometer (Jobin-Yvon, Inc.) was used for the binding assay. The fluorescently labeled PDZ domain TMR-PDZ(C338) was generated to obtain the binding affinity (K_D) of the tripeptides VVV and VWV as described previously.[14] Briefly, the TMR-PDZ protein of Dvl was dialyzed in 0.1 M potassium phosphate (pH 7.5) with 0.5 mM EDTA at least three times with a 3500 Da cutoff membrane. The fluorescently labeled TMR-PDZ was confirmed by SDS gel and mass spectroscopy. The excitation wavelength of TMR-PDZ(C338) was 552 nm (slit width = 5 nm), and the maximum emission fluorescence at 597 nm (slit width = 5 nm) was recorded during the titration of model peptides. Titration experiments were performed at 25 °C in phosphate buffer (0.1 M potassium phosphate; 0.5 mM EDTA, pH 7.5). Typically, the peptide solutions (5–200 μM) were injected into 2.0 mL of 40 nM TMR-PDZ(C338) domain. The fluorescence data were analyzed using the ORIGIN program (Microcal). The K_D value was calculated from a reciprocal plot of fluorescence intensity quenching (ΔF) against the concentration (ΔS) of peptides:

$$\frac{1}{\Delta F} = \frac{1}{F_{max}} + \frac{K_D}{F_{max}} \cdot \frac{1}{[S]} \quad (3)$$

ΔF is the change of fluorescence intensity and [S] is the peptide concentration.

4.6. Structure calculation

The ^{13}C,^{15}N-double-labeled PDZ domain of Dvl1 with the unlabeled tripeptide VWV was used for structure determination at 10 °C in 0.1 M phosphate buffer (pH 7.5). To avoid intermediate ex-

change, excess unlabeled VWV peptide was added. Tripeptide VWV resonances were assigned by using 2D [F1,F2]-double filtered TOCSY and NOESY experiments with a mixing time of 200 ms. To obtain the distance restraints, a 3D ^{13}C-F1-half-filtered and F2-edited NOESY–HSQC experiment with the ^{13}C,^{15}N-labeled PDZ domain of Dvl1 and the unlabeled tripeptide VWV with a mixing time of 200 ms was recorded (Table 1). Based on the previous assignment of the backbone and side chains of the Dvl1 PDZ domain,[9] the intermolecular NOEs between the tripeptide VWV and the Dvl1 PDZ domain were assigned. NOE cross-peak intensities were classified as strong, medium, weak, or very weak and were assigned restraints of 1.8–3.0 Å, 1.8–4.0 Å, 1.8–5.0 Å, and 1.8–6.0 Å, respectively, with appropriate pseudoatom corrections. A total of 26 intermolecular and intramolecular NOEs were identified in the complex of the Dvl1 PDZ/VWV peptide. Based on the NOEs, we then calculated the structure of the Dvl1 PDZ/VWV complex by using the simulated annealing program CNS within the HADDOCK platform.[46] The coordinates of the Dvl1 PDZ domain were taken from the X-ray structure of the *Xenopus* PDZ domain (PDB code: 1L6O), and the amino acid residues were modified to the mouse Dvl1 PDZ domain using SYBYL.[14] Two thousand initial structures were calculated. Among the final 100 water-refinement structures for the complex, we selected the 20 lowest energy conformations to represent the solution structure of the complex. The calculated structures were analyzed by the programs PROCHECK[47] and MOLMOL.[48]

4.7. Molecular dynamics simulation

MD simulation was conducted by using the Sander program in AMBER8 with the parm99 force field.[38] MD simulations were performed on a Linux cluster at the Hartwell Center at St. Jude. The starting complex structure of the Dvl1 PDZ/VWV used was the lowest energy conformation as shown in Figure 5C. Because both tripeptides VVV and VWV bound at the same site on the PDZ domain of Dvl1, we predicted that the tripeptide VVV bound to the Dvl1 PDZ domain would adopt a conformation similar to that of the VWV tripeptide. We used the coordinates of the lowest energy conformation of the PDZ/VWV complex structure as a template to generate the starting structure of the Dvl1 PDZ/VVV complex for an MD simulation: the Trp(−1) residue replaced Val(−1) residues. After neutralization with Na^+ ions, complexes were solvated in a periodic rectangular TIP3P water box with each side 9 Å away from the edge of the system.[49] The MD run included several steps as follow: (1) systems were minimized by a 1000-step steepest descent minimization followed by a 9000-step conjugated gradient minimization; (2) systems were heated from 100 K to 300 K with 5 kcal/mol harmonic restrains via a 50-ps NVT MD simulation; (3) the restraints were gradually reduced to zero via a 50-ps NPT MD simulation; and (4) trajectories were collected from a 2-ns NPT production run. The MD simulations were performed with a time step of 1 fs, and the SHAKE algorithm was used to restrain all bonds involving hydrogen. The production trajectories were saved every 2.5 ps. After simulation, the ptraj module was used to extract trajectories for further analysis.

To calculate the binding free energy, we used the MM-PBSA module implemented in the AMBER8 package without any modification; the method combines the molecular mechanical energies with the continuum solvent approaches.[39,40,50] We used 200 snapshots extracted from the last 1 ns to calculate ΔH and used 20 snapshots extracted from the last 1 ns for estimating the entropy ΔTS by normal-mode analysis. The binding free energy of complex was calculated using Eqs. (4)–(7) as below:

$$\Delta G_{\text{bind}} = G_{\text{complex}} - G_{\text{protein}} - G_{\text{ligand}} \quad (4)$$

$$G = H_{\text{gas}} + H_{\text{trans/rot}} + G_{\text{solvation}} - TS \quad (5)$$

$$G_{\text{solvation}} = G_{\text{PB}} + G_{\text{sur}} \quad (6)$$

$$G_{\text{sur}} = \gamma A + b \quad (7)$$

H_{gas} is the molecular mechanical energy in the gas phase; $H_{\text{trans/rot}}$ is the translational and rotational enthalpy, which equals $3RT$; E_{vdw} is the van der Waals contribution; E_{elec} is the electrostatic contribution; $G_{\text{solvation}}$ represents the free energy of solvation; and TS is the solute entropic contribution at temperature T. $G_{\text{solvation}}$ consists of two parts, the polar solvation energy G_{PB} and the nonpolar solvation energy G_{sur}, $G_{\text{solvation}}$ arises from the electrostatic potential between the solute and solvent, and G_{sur} is determined by the solvent-accessible area (A) and two empirical parameters, γ and b, which equal 0.00542 and 0.92, respectively.

Acknowledgments

We thank Drs. Weixing Zhang and Charles Ross for support with the NMR instruments and computer resources; Dr. Patrick Rodrigues and Mr. Robert Cassell at the Hartwell Center for Bioinformatics and Biotechnology at St. Jude Children's Research Hospital for peptide synthesis. We thank David Galloway from Scientific Editing for editorial help. This work is supported by the American Lebanese Syrian Associated Charities, by the Cancer Center Support Grant (CA21765) from the National Cancer Institute and by National Institutes of Health Grant GM081492.

References and notes

1. Wallingford, J. B.; Habas, R. *Development* **2005**, *132*, 4421.
2. Malbon, C. C.; Wang, H. Y. *Curr. Top. Dev. Biol.* **2006**, *72*, 153.
3. Uematsu, K.; Kanazawa, S.; You, L.; He, B.; Xu, Z.; Li, K.; Peterlin, B. M.; McCormick, F.; Jablons, D. M. *Cancer Res.* **2003**, *63*, 4547.
4. Uematsu, K.; He, B.; You, L.; Xu, Z.; McCormick, F.; Jablons, D. M. *Oncogene* **2003**, *22*, 7218.
5. Mizutani, K.; Miyamoto, S.; Nagahata, T.; Konishi, N.; Emi, M.; Onda, M. *Tumori* **2005**, *91*, 546.
6. Sussman, D. J.; Klingensmith, J.; Salinas, P.; Adams, P. S.; Nusse, R.; Perrimon, N. *Dev. Biol.* **1994**, *166*, 73.
7. Wong, H. C.; Mao, J.; Nguyen, J. T.; Srinivas, S.; Zhang, W.; Liu, B.; Li, L.; Wu, D.; Zheng, J. *Nat. Struct. Biol.* **2000**, *7*, 1178.
8. Capelluto, D. G.; Kutateladze, T. G.; Habas, R.; Finkielstein, C. V.; He, X.; Overduin, M. *Nature* **2002**, *419*, 726.
9. Wong, H. C.; Bourdelas, A.; Krauss, A.; Lee, H. J.; Shao, Y.; Wu, D.; Mlodzik, M.; Shi, D. L.; Zheng, J. *Mol. Cell* **2003**, *12*, 1251.
10. Schwarz-Romond, T.; Fiedler, M.; Shibata, N.; Butler, P. J.; Kikuchi, A.; Higuchi, Y.; Bienz, M. *Nat. Struct. Mol. Biol.* **2007**, *14*, 484.
11. Wang, N. X.; Lee, H. J.; Zheng, J. J. *Drug News Perspect.* **2008**, *21*, 137.
12. Cheyette, B. N.; Waxman, J. S.; Miller, J. R.; Takemaru, K.; Sheldahl, L. C.; Khlebtsova, N.; Fox, E. P.; Earnest, T.; Moon, R. T. *Dev. Cell* **2002**, *2*, 449.
13. London, T. B.; Lee, H. J.; Shao, Y.; Zheng, J. *Biochem. Biophys. Res. Commun.* **2004**, *322*, 326.
14. Shan, J.; Shi, D. L.; Wang, J.; Zheng, J. *Biochemistry* **2005**, *44*, 15495.
15. Fujii, N.; You, L.; Xu, Z.; Uematsu, K.; Shan, J.; He, B.; Mikami, I.; Edmondson, L. R.; Neale, G.; Zheng, J.; Guy, R. K.; Jablons, D. M. *Cancer Res.* **2007**, *67*, 573.
16. Shan, J.; Zheng, J. J. *J. Comput. Aided Mol. Des.* **2008**, doi: 10.1007/s10822-008-9236-1.
17. Bhutia, S. K.; Maiti, T. K. *Trends Biotechnol.* **2008**, *26*, 210.
18. Hong, F.; Ming, L.; Yi, S.; Zhanxia, L.; Yongquan, W.; Chi, L. *Peptides* **2008**, *29*, 1062.
19. Rifai, Y.; Elder, A. S.; Carati, C. J.; Hussey, D. J.; Li, X.; Woods, C. M.; Schloithe, A. C.; Thomas, A. C.; Mathison, R. D.; Davison, J. S.; Toouli, J.; Saccone, G. T. *Am. J. Physiol. Gastrointest. Liver Physiol.* **2008**, *294*, G1094.
20. Kannengiesser, K.; Maaser, C.; Heidemann, J.; Luegering, A.; Ross, M.; Brzoska, T.; Bohm, M.; Luger, T. A.; Domschke, W.; Kucharzik, T. *Inflamm. Bowel. Dis.* **2008**, *14*, 324.
21. Charnley, M.; Moir, A. J.; Douglas, C. W.; Haycock, J. W. *Peptides* **2008**, *29*, 1004.
22. Yao, Z.; Lu, R.; Jia, J.; Zhao, P.; Yang, J.; Zheng, M.; Lu, J.; Jin, M.; Yang, H.; Gao, W. *Peptides* **2006**, *27*, 1167.
23. Blodgett, J. A.; Thomas, P. M.; Li, G.; Velasquez, J. E.; van der Donk, W. A.; Kelleher, N. L.; Metcalf, W. W. *Nat. Chem. Biol.* **2007**, *3*, 480.
24. Lee, H.-J.; Park, H.-M.; Lee, K.-B. *Biophys. Chem.* **2007**, *125*, 117.
25. Eker, F.; Cao, X.; Nafie, L.; Schweitzer-Stenner, R. *J. Am. Chem. Soc.* **2002**, *124*, 14330.
26. Schweitzer-Stenner, R.; Eker, F.; Perez, A.; Griebenow, K.; Cao, X.; Nafie, L. A. *Biopolymers* **2003**, *71*, 558.

27. Eker, F.; Griebenow, K.; Schweitzer-Stenner, R. *J. Am. Chem. Soc.* **2003**, *125*, 8178.
28. Eker, F.; Griebenow, K.; Cao, X.; Nafie, L. A.; Schweitzer-Stenner, R. *Proc. Natl. Acad. Sci. U.S.A.* **2004**, *101*, 10054.
29. Eker, F.; Griebenow, K.; Cao, X.; Nafie, L. A.; Schweitzer-Stenner, R. *Biochemistry* **2004**, *43*, 613.
30. Motta, A.; Reches, M.; Pappalardo, L.; Andreotti, G.; Gazit, E. *Biochemistry* **2005**, *44*, 14170.
31. Shi, Z.; Chen, K.; Liu, Z.; Ng, A.; Bracken, W. C.; Kallenbach, N. R. *Proc. Natl. Acad. Sci. U.S.A.* **2005**, *102*, 17964.
32. Vaccaro, P.; Dente, L. *FEBS Lett.* **2002**, *512*, 345.
33. Pellecchia, M.; Sem, D. S.; Wuthrich, K. *Nat. Rev. Drug Disc.* **2002**, *1*, 211.
34. Skelton, N. J.; Koehler, M. F.; Zobel, K.; Wong, W. L.; Yeh, S.; Pisabarro, M. T.; Yin, J. P.; Lasky, L. A.; Sidhu, S. S. *J. Biol. Chem.* **2003**, *278*, 7645.
35. Appleton, B. A.; Zhang, Y.; Wu, P.; Yin, J. P.; Hunziker, W.; Skelton, N. J.; Sidhu, S. S.; Wiesmann, C. *J. Biol. Chem.* **2006**, *281*, 22312.
36. Runyon, S. T.; Zhang, Y.; Appleton, B. A.; Sazinsky, S. L.; Wu, P.; Pan, B.; Wiesmann, C.; Skelton, N. J.; Sidhu, S. S. *Protein Sci.* **2007**, *16*, 2454.
37. Schapira, M.; Totrov, M.; Abagyan, R. *J. Mol. Recognit.* **1999**, *12*, 177.
38. AMBER 8, Scripps Research Institute, La Jolla, CA., 2004.
39. Wang, J.; Morin, P.; Wang, W.; Kollman, P. A. *J. Am. Chem. Soc.* **2001**, *123*, 5221.
40. Wang, W.; Donini, O.; Reyes, C. M.; Kollman, P. A. *Annu. Rev. Biophys. Biomol. Struct.* **2001**, *30*, 211.
41. Loughlin, W. A.; Tyndall, J. D.; Glenn, M. P.; Fairlie, D. P. *Chem. Rev.* **2004**, *104*, 6085.
42. Fuh, G.; Pisabarro, M. T.; Li, Y.; Quan, C.; Lasky, L. A.; Sidhu, S. S. *J. Biol. Chem.* **2000**, *275*, 21486.
43. Wiedemann, U.; Boisguerin, P.; Leben, R.; Leitner, D.; Krause, G.; Moelling, K.; Volkmer-Engert, R.; Oschkinat, H. *J. Mol. Biol.* **2004**, *343*, 703.
44. Song, E.; Gao, S.; Tian, R.; Ma, S.; Huang, H.; Guo, J.; Li, Y.; Zhang, L.; Gao, Y. *Mol. Cell Proteomics* **2006**, *5*, 1368.
45. Delaglio, F.; Grzesiek, S.; Vuister, G. W.; Zhu, G.; Pfeifer, J.; Bax, A. *J. Biomol. NMR* **1995**, *6*, 277.
46. Dominguez, C.; Boelens, R.; Bonvin, A. M. *J. Am. Chem. Soc.* **2003**, *125*, 1731.
47. Laskowski, R. A.; Rullmannn, J. A.; MacArthur, M. W.; Kaptein, R.; Thornton, J. M. *J. Biomol. NMR* **1996**, *8*, 477.
48. Koradi, R.; Billeter, M.; Wuthrich, K. *J. Mol. Graphics* **1996**, *14*, 51.
49. Jorgensen, W. L.; Chandrasekhar, J.; Madura, J. D.; Klein, M. *J. Chem. Phys.* **1983**, *79*, 926.
50. Orozco, M.; Luque, F. J. *Chem. Rev.* **2001**, *101*, 203.